JOURNAL OF MATERIALS SCIENCE 37 (2002) 2023–2029

SiC nanorods prepared from SiO and activated carbon

Y. H. GAO*, Y. BANDO, K. KURASHIMA, T. SATO
Advanced Materials Laboratory and Nanomaterials Laboratory, National Institute for Materials Science (NIMS), Namiki 1-1, Tsukuba, Ibaraki 305-0044, Japan
E-mail: GAO.Yihua@nims.go.jp

SiC nanorods with 20–100 nm diameter and 10–100 μm length were synthesized by reaction between SiO and amorphous activated carbon (AAC) at 1380°C. Microstructural characterization of the SiC nanorods was carried out by high resolution transmission electron microscopy (HRTEM) and energy dispersive spectroscopy (EDS). The SiC nanorods grow on either a chain or from facets of SiC nanoparticles. They are usually straight and preferentially orientated along the [111] direction. Branching phenomenon exists for these nanorods. Typical SiC nanorod tip was analyzed by HRTEM image and EDS analysis. Based on an experimental analysis, a formation mechanism is proposed to explain the microstructural characterization of the SiC nanorods.

1. Introduction

Silicon carbide (SiC) is a material of great technological interest for devices based on its unique properties, e.g. high hardness, high thermal stability, high chemical stability and large band gap [1]. When SiC is fabricated as one dimensional nanorods, they have unique optical properties [2] together with unique mechanical properties [3]. For example, the photoluminescence emission is in the blue range at room temperature and, with respect to their mechanical properties, the elastic constant reaches the theoretical value of 600 GPa for [111]-oriented SiC. Carbothermal reduction is a useful synthesis method for the synthesis of SiC nanorods, and two kinds of reduction methodologies have been developed successfully. One method involves reduction of sol-gel-derived silica xerogels containing carbon nanoparticles [4]. In this method, it is believed that large quantities of SiC nuclei from on carbon nanoparticles and that SiC nanorods together with amorphous SiO_2 wrapping layers grow along the [111] direction via a vapor-vapor (VV) reaction mechanism. The other method is direct carbothermal reduction of halide, i.e. SiI_4 [5] or silica and silicon, i.e. $SiO_2 + Si$ [2], where the reductant is carbon nanotubes (CNTs). SiC nanorods obtained by this method are ~20 nm in diameter [5] and have growth axes projecting along [111]. It is believed that the SiC nanorods are converted from the CNTs, which act as the template for formation of SiC nanorods.

The two methods have some disadvantages which may limit the fabrication and application of SiC nanorods. The first method has a complicated synthesis procedure and the synthesized SiC nanorods usually have amorphous wrapping layers of SiO_2, while the second needs expensive CNTs as a reductant. To overcome these disadvantages, a direct carbothermal reduction method is adopted in our experiment, where SiO is reduced by amorphous activated carbon (AAC). The method demonstrates the possibility for industrial manufacture of SiC nanorods.

In general, experimental conditions are important for growth of materials, and microstructural characteristics are important clues as to the growth mechanism of the obtained materials. In our investigations, we paid much attention to experimental analysis and microstructural characteristics of the SiC nanorods, including: the morphology, the length, the diameter, the growth axis direction and the tip morphology and compositions. Based on an analysis of experimental conditions, a mechanism different from the template mechanism [2, 5] is proposed to explain the formation of SiC nanorods with the microstructural characterization.

2. Experimental

The SiC nanorods were obtained in a vertical reactor, which consists of a clear fused-quartz tube 500 mm in length, 120 mm in diameter and 2.5 mm in thickness. The fused-quartz tube contains an inductively heated cylinder of high purity graphite, which is 70 mm in length, 45 mm in outer diameter and 35 mm in inner diameter. A graphite (or BN) crucible, which is ~20 mm in diameter and ~20 mm in height, was put in the cylinder. The graphite crucible was fed with the reactants, 99.9% purity of SiO and amorphous activated carbon (AAC) powder, where the AAC was placed on top of the SiO powder. The weight ratio between SiO and AAC is 3 : 1. These materials are heated at

*Author to whom all correspondence should be addressed.

1380°C for 2 hours, at which temperature the SiO vaporizes. During the heating process, pure Ar was introduced to protect the reactants to prevent oxidation. Following reaction, the product was collected at the crucible bottom. Transmission electron microscope (TEM) specimen was obtained by dispersing the product into alcohol and placing the dispersion drop onto a Cu mesh grid. The TEM specimen was examined in a 300 kV field emission analytical electron microscope (JEM-3000F) equipped with an energy dispersive spectrometer (EDS).

3. Results

The AAC, as shown in the scanning electron microscopy (SEM) micrograph Fig. 1a, consists of many large C fragments 1–100 μm in size. The TEM micrograph of Fig. 1b and diffraction pattern Fig. 1c show many tiny amorphous C nanoparticles ∼10 nm in size on the surface of the C fragments.

SiC nanoparticles and nanorods are the two kinds of materials in the product. It is estimated that the yield of nanorods is about 10%. Fig. 2 shows the morphology of some nanorods and their diffraction pattern inset, which can be indexed according to the β-SiC structure. The SiC nanorods typically have diameters of 20–100 nm and lengths of 10–100 μm. The SiC nanorods usually connect to either chains or fragments of SiC nanoparticles 20–100 nm in size, as shown in Fig. 3a–c. In the SiC nanoparticles, only Si, C and small quantities of O can be detected using EDS analysis.

The nanorods are usually straight, as shown in Fig. 4a. Each nanorod has a preferential growth axis parallel to the [111] direction. This axis orientation was found to be constant along the length of the nanorod. A high density of striations exists in the nanorods. Fig. 4b is the dark field image of the rod indicated by an arrow in Fig. 4a using the circled diffraction spots in Fig. 4c. The analysis of Figs 4 shows that the striations normal to the axes in Fig. 4a are stacking faults normal to the [111] direction.

For the straight SiC nanorods with [111] growth axis orientation, there is an interesting branching phenomenon, as shown in Fig. 5. The upper SiC nanorod grows on the bottom one at an angle of 70°, and some stacking faults "SF" extend from the bottom to the upper one. Beside the extending stacking faults, there is an intermediate region delineated by two lines. The line parallel to the stacking faults denoted "SF" corresponds

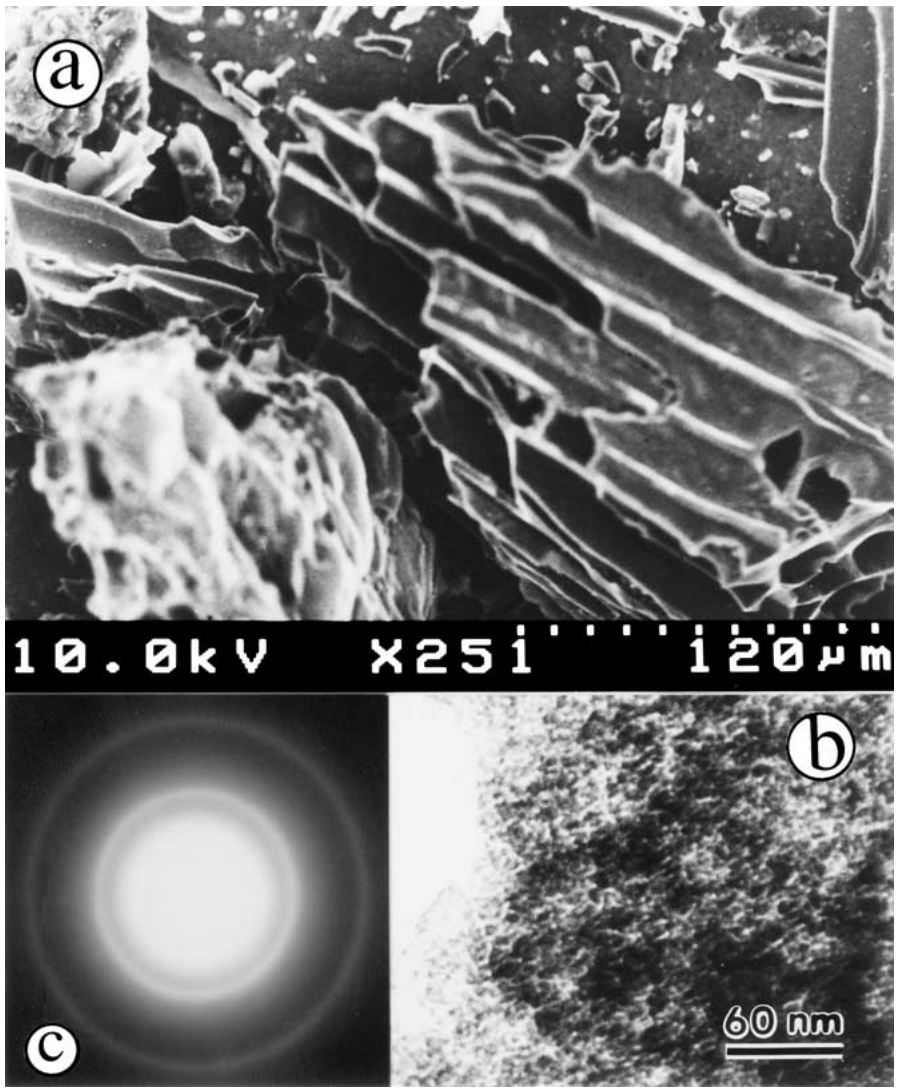

Figure 1 (a) A scanning electron microscopy image of activated carbon. (b) The morphology of the numerous C nanoparticles on a C fragment. (c) The electron diffraction pattern of the C agglomerate in (b). It shows that the activated carbon is amorphous.

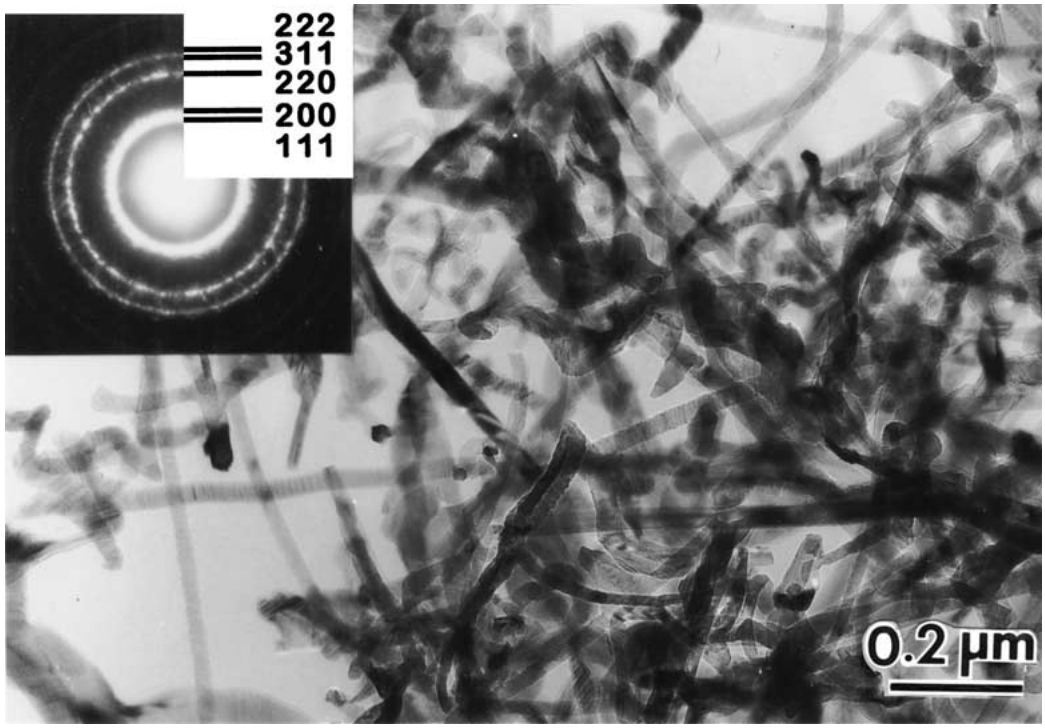

Figure 2 Micrograph showing SiC nanorods formed in the product. The inset is the diffraction pattern of the nanorods. The diffraction pattern can be indexed as β-SiC.

to the (111) plane of the bottom one, while the other line normal to the $[11\bar{1}]$ direction corresponds to the $(11\bar{1})$ plane of the branching nanorod.

Fig. 6a shows an HRTEM image of the typical tip of a straight SiC nanorod. The inset is its $[1\bar{1}0]$ diffraction pattern. On the tip, there is a thin SiC region denoted "C" and a thin amorphous layer denoted "A". The thin region "C" has the same orientation as that of the left thicker region with a darker contrast. Its contrast reveals that it becomes gradually thinner from left to right. The thin amorphous layer "A" with 1–3 nm thickness contains Si, C and a small amount of O, as shown in its EDS spectrum, Fig. 6b. For comparison, the EDS spectrum of the dark region is shown in Fig. 6c.

4. Discussion

In the graphite (or BN) crucible, there are C nanoparticles on AAC pieces, SiO powder, and SiO vapor when SiO vaporizes at 1380°C. Between these materials, two kinds of reaction can be defined. Initially, SiO vapor comes to the C nanoparticle-sites on the AAC fragments and reacts with them as follows,

$$\mathrm{SiO(vapor)} + 2\mathrm{C(nanoparticles)} \rightarrow \mathrm{SiC(nanoparticles)} + \mathrm{CO(vapor)} \quad (1)$$

As reaction occurs on C nanoparticle-sites, the C nanoparticles serve as templates, and the synthesized SiC nanoparticles should be similar in size to the C nanoparticles. Reaction (1) is a vapor-solid (VS) reaction. Since the starting C nanoparticles on AAC fragments connected together, reaction (1) can lead to a chain of SiC nanoparticles as shown in Fig. 3a and c. In fact, the C nanoparticles in reaction (1) act as both reductant and template for the formation of the SiC nanoparticles. Using a template mechanism, *Han* explained the formation of one-dimensional SiC nanorods as the result of the reaction, $\mathrm{SiO(vapor)} + 2\mathrm{C(CNTs)} \rightarrow \mathrm{SiC(nanorods)} + \mathrm{CO(vapor)}$, occurring on one-dimensional CNTs [2]. However, the formation of our SiC nanorods cannot be readily explained by a template mechanism via reaction (1). This is because reaction (1) on the C nanoparticles-sites results in the formation of SiC nanoparticles only when the C nanoparticles serve as a template. Secondly, the SiO powder can react with AAC pieces at the SiO/AAC contact interface and results in SiC particles through a reaction,

$$\mathrm{SiO(interfacial\ powder)} + 2\mathrm{C(interfacial\ AAC\ pieces)} \rightarrow \mathrm{SiC(particles)} + \mathrm{CO(vapor)} \quad (2)$$

We have performed another experiment to confirm this reaction.

The above analysis illustrates that reactions (1) and (2) between SiO and C do not result in the formation of SiC nanorods. In addition, the formation of the nanorods is not realized by a metallic catalyst mechanism [6] because no catalyst exists in our starting materials. Since SiC nanorods consist of Si and C, we should search for other possible reactions providing Si and C species. In our experiment crucible, another reaction we have not mentioned may occur to provide Si and C species as follows.

$$\mathrm{SiO(vapor)} + 3\mathrm{CO(vapor)} \rightarrow \mathrm{SiC(solid)} + 2\mathrm{CO_2(vapor)} \quad (3)$$

It is a vapor phase reaction between SiO and CO. This reaction was stimulated by the CO vapor generated

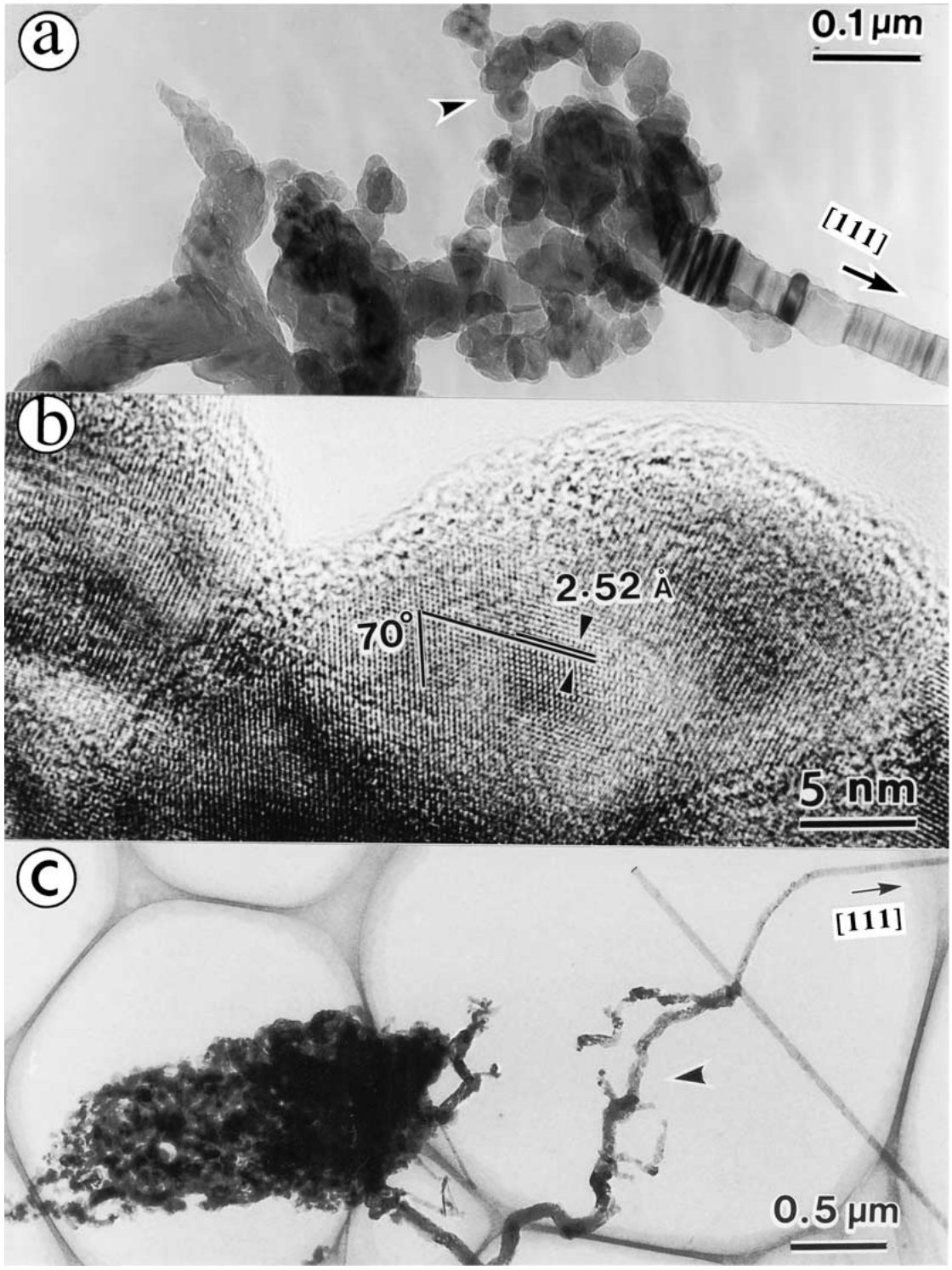

Figure 3 (a) Morphology of a straight SiC nanorod connecting a chain of SiC nanoparticles. (b) An HRTEM image of a nanoparticle in this chain of SiC nanoparticles. (c) Morphology of a straight nanorod connecting SiC nanoparticles via a curved region indicated by an arrow.

from reaction (1), while the generated CO_2 vapor can taken into the following reaction

$$CO_2(\text{vapor}) + C \rightarrow 2CO(\text{vapor}) \quad (4)$$

leading to the formation of CO vapor. Reaction (3) can occur under a supersaturated condition of CO vapor in a localized space. This supersaturation is realized through the following described mode. 3 mol of CO vapor can lead to 2 mol of CO_2 vapor via reaction (3), while 2 mol of CO_2 vapor result in 4 mol of CO vapor via reaction (4). Conversely, the generated 4 mol of CO will be taken into reaction (3) and lead to 8/3 mol of CO_2 vapor via reaction (3), and then 16/3 mol of CO vapor via reaction (4). Obviously, reactions (3) and (4) have a positive feedback characteristic to each other and lead to a supersaturation of CO vapor ultimately. Under this supersaturation. SiC nanorods were generated, as shown schematically in Fig. 7. As reaction (3) does not lead to nanorods before reaching

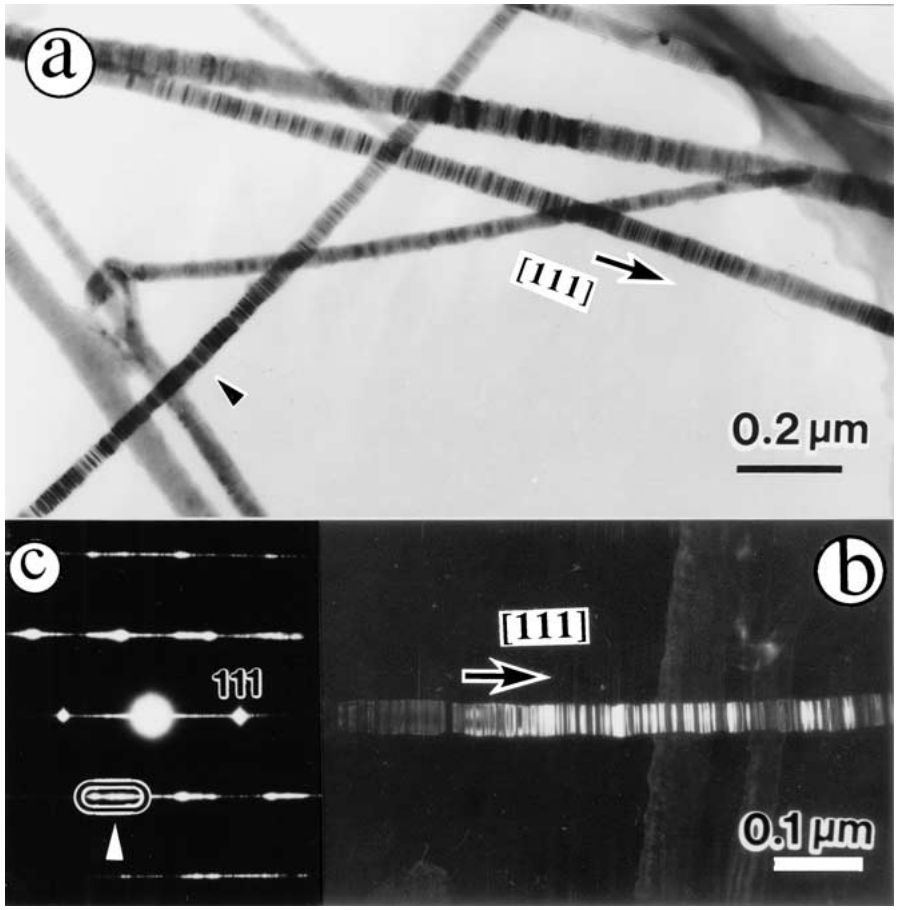

Figure 4 (a) Micrograph showing straight SiC nanorods. In each nanorod, there is a high density of striations normal to the axis; (b) A dark field image of a straight nanorod indicated by an arrow in (a); (c) [1$\bar{1}$0] diffraction pattern of the straight nanorod in (b).

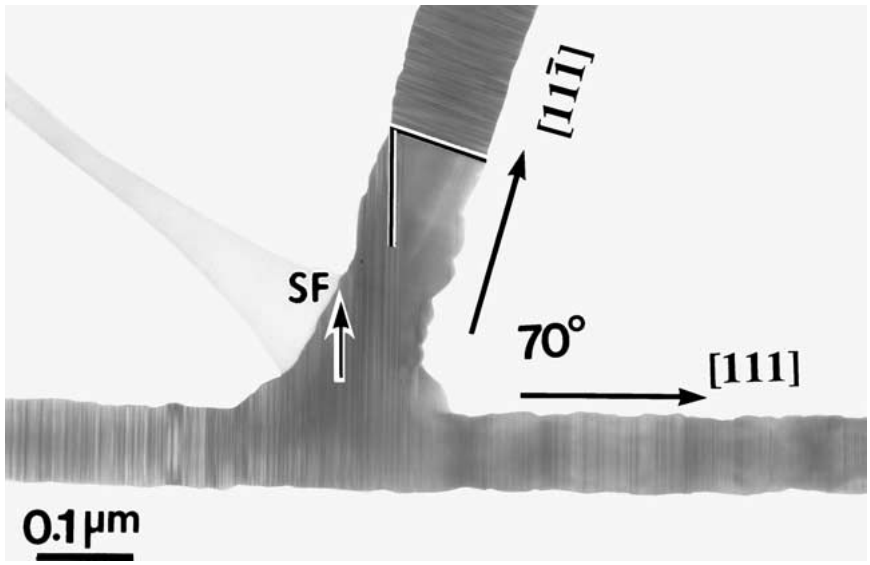

Figure 5 Morphology of the upper SiC nanorod growing on the bottom one at a 70° angle. Stacking faults denoted "SF" extend from the bottom one to the upper one.

supersaturation, and SiC nanorods can only grow under a supersaturation condition, their yield was limited below 100% in the product. The growth under supersaturation is a kinetic growth leading to needle-like crystals [7]. The growth along the needle-axis is unimpeded, while growth normal to its axis is impeded. In general, its axis is preferentially normal to the lowest energy plane, which is the (111) plane for SiC. When the needle-like crystal starts its growth from a SiC nanoparticle, the SiC nanoparticle serves as a SiC nucleus and controls the diameter of the needle-like crystal. From the above analysis, we propose three growth processes of the SiC nanorods in our experiment. (a) The SiC nanorods start their growth from SiC nanoparticles with

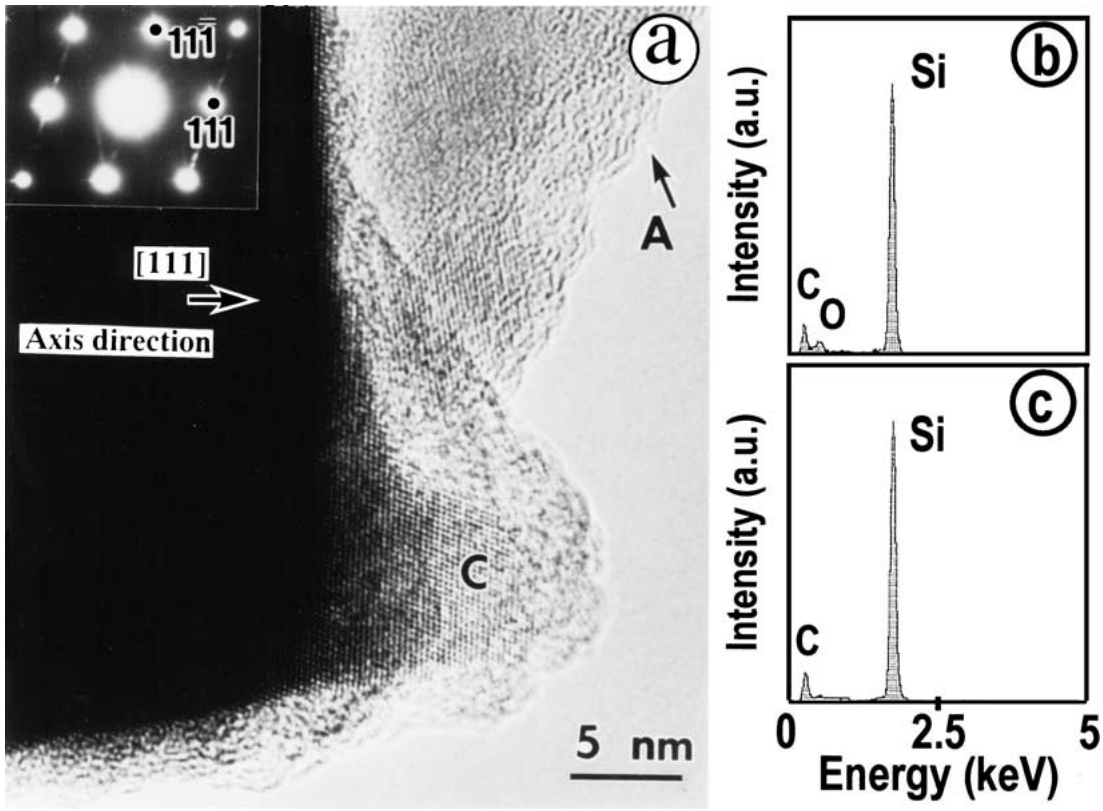

Figure 6 (a) HRTEM image of a SiC nanorod tip and its corresponding [$1\bar{1}0$] diffraction pattern. On the tip, there is a thin SiC layer "C" and an amorphous thin layer "A". (b) EDS spectra of the thin amorphous layer "A" in (a). (c) EDS spectra of the dark region in (a). In (b) and (c), the peaks are Kα lines (0.28 ke V, 0.53 keV and 1.74 keV) of C, O and Si, respectively.

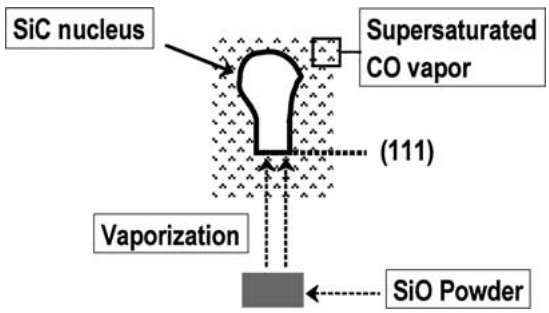

Figure 7 Growth diagram of a SiC nanorod. Under supersaturation of CO atmosphere, SiC molecular deposits continuously on (111) plane when SiO vaporizes onto this plane, leading to growth of SiC nanorod.

the similar diameter; (b) The growth of SiC nanorods is then kinetically controlled via reaction (3) at supersaturation of CO vapor; (c) Once the supersaturation condition stops, the growth of SiC nanorods is terminated.

In terms of the supersaturation concept, we can understand the curved SiC nanorods in Fig. 3, stacking faults in SiC nanorods and the branching phenomenon in Fig. 5. Under this supersaturation condition, (a) SiC [7] can also grow along the direction normal to [111]. Therefore, SiC nanorods can grow along a composite direction of [111] and the direction normal to [111]. When the two growth rates along the two directions fluctuate with a disturbance of the kinetic growth condition, the growth direction changes, and a curved SiC nanorod results; (b) The growth of SiC nanorods preferentially along the [111] direction can be considered as a continuous deposition of Si and C layers on the "seeding" surface (111) plane of the parent SiC nanoparticles layer-by-layer. The deposition of Si and C layers can have stacking sequences of either "$\ldots A_{Si}A_CB_{Si}B_CA_{Si}A_C\ldots$" or "$\ldots.A_{Si}A_CB_{Si}B_CC_{Si}C_CA_{Si}A_C\ldots$". When the two sequences coexist in a SiC nanorod, stacking faults result. This coexistence of the two sequences in a SiC nanorod is beneficial to the increase of entropy and decrease of Gibbs energy of SiC [1]; (c) Dendritic growth is a general phenomenon under supersaturation [7], thus the branching phenomenon as shown in Fig. 5 results. The stacking faults denoted "SF" grow out from the bottom nanorod and serve as a nucleus [8], from which the new nanorod grows. The join region has two of the lowest energy planes. One is the (111) plane. It inherits the crystallographic orientation of the bottom SiC nanorod. The other is the ($11\bar{1}$) plane. On the ($11\bar{1}$) plane, the upper nanorod grows along the [$11\bar{1}$] direction.

Nevertheless, the microstructure of the SiC tip in Fig. 6 indicates that the kinetic growth has stopped. The thin region "C" forms during the final kinetic growth stage of the SiC nanorod when few Si or C species are being provided via reaction (3). However, the growth of the amorphous thin layer "A" in Fig. 6, which contains a mixture of Si, C and O, cannot be readily explained directly in terms of reaction (3). This layer may form by oxidation of the thin SiC tip when SiC nanorods are exposed to air. It may also be caused by another mechanism. Since the kinetic growth stops at the SiC tip, the amorphous layer grows at a condition approaching

thermodynamic equilibrium. The growth may occur at lower temperature during cooling once the heating is finished as in the following reaction,

$$3SiO(vapor) + CO(vapor) \rightarrow SiC(solid) + 2SiO_2(solid) \quad (5)$$

This reaction (5) leads to decrease in enthalpy and Gibbs energy at temperatures below 900°C [9].

5. Conclusions

SiC nanorods with 20–100 nm diameter and 10–100 μm length have been synthesized by a reaction between SiO and amorphous activated carbon (AAC) at 1380°C. The synthesized SiC nanorods usually grow on a chain or piece of SiC nanoparticles. The SiC nanorods are generally straight and have a preferential axis orientation parallel to the [111] direction. A branching phenomenon exists in the nanorods. On a typical tip of the straight SiC nanorod, there is a thin amorphous layer 1–3 nm thick, which consists of Si, C and a small quantity of O. It is believed that the growth of the SiC nanorods starts from the initial SiC nuclei forming in the reaction process between SiO vapor and C nanoparticles on the AAC fragments, grow then along the [111] direction via the reaction between SiO and CO vapor at supersaturation and then ends with the formation of SiC tips when supersaturation of SiO and CO stops.

Acknowledgments

This work was supported by the Japan Science and Technology Corporation (JST).

References

1. A. R. VERMA and P. KRISHNA, "Polymorphism and Polytypism in Crystals" (John Wily and Sons, New York, 1966) p. 63, 97.
2. W. Q. HAN, S. S. FAN, Q. Q. LI, W. J. LIANG, B. L. GU and D. P. YU, *Chem. Phys. Lett.* **265** (1997) 374.
3. E. W. WONG, P. E. SHEEHAN and C. M. LIEBER, *Science* **277** (1997) 1971.
4. G. W. MENG, L. D. ZHANG, C. M. MO, S. Y. ZHANG, Y. QIN, S. P. FENG and H. J. LI, *J. Mater. Res.* **13** (1998) 2533.
5. H. J. DAI, E. W. WONG, Y. Z. LU, S. S. FANG and C. M. LIEBER, *Nature (London)* **375** (1995) 769.
6. R. S. WAGNER and W. C. ELLIS, *Appl. Phys. Lett.* **4** (1964) 89.
7. B. R. PAMPLIN, "Crystal Growth," 2nd ed. (Pergamon Press, 1980) p. 58.
8. A. C. ZETTLEMOYER, "Nucleation" (Marcel Dekker, 1969) p. 337.
9. M. W. CHASE, JR., C. A. DAVIES, J. R. DOWNEY, JR., D. J. FRURIP, R. A. MCDONALS and A. N. SYVERUD, "JANAF Thermochemical Tables," 3rd ed. (American Chemical Society and the American Institute of Physics, 1985).

Received 29 March
and accepted 14 January 2002